RESEARCH PAPER

Intranasal Nanoparticle Delivery System for Improved Cognitive Function in Alzheimer's Disease

D. Varun[1], Ravindra Jallu[2], Shaik Farahan Subahan[3], Donakanti Rachana[4], Umarov Sherzojon Usmonovich[5], Mashrab Yusupov Ismatillovich[6], Jaya Raju Nandikola[7] and D. Naga Latha[8*]

[1]*Department of Pharmaceutics, Pulla Reddy Institute of Pharmacy. Hyderabad - 502313, Telangana, India.*
[2]*Department of Pharmacy Practice, Pulla Reddy Institute of Pharmacy. Hyderabad - 502313, Telangana, India.*
[3]*Department of Pharmacy Practice, Vijaya Institute of Pharmaceutical Sciences for Women, Enikepadu, Vijayawada Rural, Vijayawada-521108, Andhra Pradesh.*
[4]*University of New Haven, 300 Boston Post Rd, West Haven, Connecticut 06516, USA*
[5]*Department of Social Sciences, Fergana Medical Institute of Public Health, Yangi Turon 2A, Fergana-150100, Uzbekistan.*
[6]*Department of Microbiology, Virology and Immunology, Samarkand State Medical University, 140104 Amir Temur 18A, Samarkand, Uzbekistan.*
[7]*International European University, Malta Campus, Malta, Europe.*
[8]*Department of Pharmacy Practice, Pulla Reddy Institute of Pharmacy. Hyderabad - 502313, Telangana, India.*

Corresponding Author:
Dr. D. Naga Latha,
Associate Professor & HOD,
Department of Pharmacy Practice, Pulla Reddy Institute of Pharmacy. Hyderabad - 502313, Telangana, India.
E-mail: latha.dhulipalla9@gmail.com

ABSTRACT
Alzheimer's disease (AD) is a progressive neurodegenerative disorder marked by cognitive dysfunction, memory loss, and behavioral changes. Importantly, one of the most significant obstacles in AD treatment is the limited blood–brain permeability of therapeutic entities and consequently resulting ineffective drug transport to the central nervous system (CNS). The development of nanotechnology-based delivery systems has opened new avenues for effective brain-targeting of therapeutic agents. Of these, intranasal nanoparticle delivery systems provide both a less-invasive drug administration that can promote the targeting of drugs towards CNS through trigeminal or olfactory neural pathway without passing BBB. The current study describes the design and evaluation of a nanoparticle delivery system for intranasal administration that can enhance cognitive function in Alzheimer's disease. Biodegradable polymeric nanoparticles encapsulated neuroprotective therapeutic agents. The formulation was characterized regarding particle size, zeta potential, drug loading efficiency and stability. Drug release profile and nasal mucosal permeability were studied through in vitro release studies and ex vivo permeation analyses respectively. The findings showed that the developed nanocarriers exhibited improved targeting to the brain, sustained release of drugs, enhanced neuronal protection and remarkable improvements in cognitive performance versus traditional routes of administration. These results suggest that intranasal nanoparticle delivery systems represent a promising therapeutic avenue in the treatment of Alzheimer's disease by improving drug bioavailability and brain distribution. This strategy needs to be translated into therapies for patients with neurodegenerative diseases, which will require additional clinical exploration.

Keywords: *Alzheimer's disease; Intranasal drug delivery; Nanoparticles; Brain targeting; Cognitive enhancement; Blood–brain barrier; Neurodegeneration; Nanomedicine*
How to cite this article: *Varun D, Jallu R, Subahan SF, Rachana D, Usmonovich US, Ismatillovich MY, Nandikola JR, Latha DN*, Intranasal Nanoparticle Delivery System for Improved Cognitive Function in Alzheimer's Disease..Int J Drug Deliv Technol. 2026; 16(11s): 40-50; DOI: 10.25258/ijddt.16.11s.5
Source of support: Nil.
Conflict of interest: None

INTRODUCTION

Alzheimer's disease (AD) is the most common type of dementia, and a leading global health challenge owing to its progressive nature and rising incidence among the elderly population. Clinical manifestations of AD include aberrations in neuronal death, synaptic damage or dysregulation, and build-up of disease hallmarks such as amyloid-β plaques and misfolded neurofibrillary tangles (NFT) containing hyperphosphorylated tau protein. These pathological changes result in cognitive decline, memory loss and impaired functioning in daily life[1,2].

Despite positive results in 25–30% of clinical trials investigating new AD therapeutic strategies, no therapies effectively slow the progression of cognitive impairment and dementia associated with AD. The current pharmacological therapies for AD, namely cholinesterase inhibitors and NMDA receptor antagonists, primarily provide symptomatic relief rather than altering the natural

**Author for Correspondence: latha.dhulipalla9@gmail.com*

course of the disease. The blood-brain barrier (BBB) poses as a large challenge to the design of efficacious AD treatments, preventing numerous drugs from reaching their targets inside of the brain. Consequently, many promising drugs fail to reach adequate concentrations at the desired site of action within the CNS[3,4].

Nanotechnology has been an effective strategy for enhanced drug delivery accessing the brain. Due to their unique physicochemical properties such as small particle size, large surface area and ability to be functionalized with targeting ligands, Nanoparticles have appeared as very promising drug carriers for cancer therapy. These features enable nanoparticles to improving drug stability, prolonged blood circulation time and targeted delivery to target tissues. Nanoparticle-based drug delivery systems have also demonstrated the potential to enhance therapeutic efficacy and lower systemic toxicity in neurological disorders[5,6].

Intranasal delivery holds great promise in brain targeting among several drug administration routes. In particular, the nasal cavity offers a means of bypassing the blood brain barrier (BBB) via olfactory and trigeminal nerve pathways to access the CNS. It is a non-invasive, rapid, and comfortable route; hence highly desirable for chronic neurological conditions. The high absorption efficiency, combined with the merit of nanoparticle technology, shows great potential in improving brain distribution and therapeutic effect[7,8].

Intranasal nanoparticle systems have been shown to enable sensory delivery of neuroprotective compounds, peptides and small molecules into the brain in recent studies. Such systems enhance drug stability, shield therapeutic agents from enzymatic degradation and allow extended-release of drugs. In addition, the surface modifications of nanoparticles can improve the mucoadhesion and cellular uptake, which thus enhances the drug absorption across nasal mucosa[9,10].

To respond to this need, the present study has developed and evaluated an intranasal nanoparticle delivery system that targets cognitive function enhancement in Alzheimer's disease. The study involved formulation and characterization of nanoparticles, drug release behavior from the formulated particles, nasal permeation studies, and in vivo cognitive assessment in an experimental animal model of Alzheimer disease. This study aims to develop a novel approach for overcoming the drawbacks of traditional treatment methods and improving therapeutic efficacy in patients suffering from neurodegenerative diseases through the combination of nanotechnology and intranasal drug administration[11,12].

Materials

Materials used in this study included the biodegradable polymers, therapeutic agent with neuroprotective activity, stabilizers, and necessary analytical reagents for nanoparticle formulation and characterization. PLGA and chitosan have been used as the major polymeric materials to produce nanoparticles because of their biocompatibility, biodegradability, and increasing drug loading. Rivastigmine for cognitive enhancement was ordered from a licensed pharmaceutical supplier. Polysorbate-80 and others were used as surfactants to stabilize nanoparticle dispersions and enhance particle uniformity. Analytical grade solvents such as ethanol and acetone were employed during nanoparticle synthesis. In vitro release studies were performed using phosphate buffer saline (PBS) as the dissolution medium. Ethical approval was attained prior to harvesting nasal mucosal tissues for ex vivo permeation studies, which were obtained from freshly sacrificed laboratory animals. Reagents and chemicals All reagents and chemicals used in the present study were of analytical or pharmaceutical grade and utilized without any further purification. In vivo studies employed experimental animals, which were adult Wistar rats housed in a controlled laboratory animal facility with constant normal diet and water access ad libitum[13,14].

Methods

Fourier Transform Infrared (FTIR) spectroscopy

The compatibility of the drug (Rivastigmine) and formulation polymers were assessed using FTIR spectroscopy. The FTIR spectra of pure drug, polymers (PLGA and chitosan), physical mixture and drug-loaded nanoparticles were recorded using PerkinElmer FTIR Spectrometer.

Samples were combined with potassium bromide (KBr) and pressed into pellets. The spectra were acquired between 4000 and 400 cm^{-1} with a resolution of 4 cm^{-1}. The spectra obtained were compared to determine characteristic peaks and explore any possible interactions between the drug and polymers. The characteristic peaks of the drug in the nanoparticle formulation confirmed that no significant chemical interaction occurred and that the other excipients were well compatible[14].

Preparation of Nanoparticle Formulation

Polyvinyl alcohol (PVA, 87–89% hydrolyzed) purchased from Sigma Aldrich was utilized to prepare nanoparticles by employing the nanoprecipitation method. For this approach, the polymer and Rivastigmine were solubilized in an organic solvent to prepare the organic phase, while a stabilizer was included in another aqueous phase. Under continuous magnetic stirring, The organic phase was slowly added dropwise into the aqueous phase. The fast evaporation of the solvent gave rise to nanoparticles. The solvent was evaporated under reduced pressure to obtain stable nanoparticles. The suspension was then centrifuged to separate unencapsulated drug and washed with distilled water for obtaining purified nanoparticles[15].

Characterization of Particles Size and Zeta Potential

Dynamic light scattering (DLS) was used to ascertain the particle size distribution and surface charge of the nanoparticles. A suspension of diluted nanoparticles was placed inside a sample cell and then the measurements were recorded at room temperature. Although this information is provided by nanoparticle characterization based on particle size distribution, zeta potential measurement information serves to show the stability of the colloidal system. Generally, high zeta potential values are typical of stable nanoparticle systems, as this indicates that there is significant electrostatic repulsion between particles[16].

Drug Loading and Encapsulation Efficiency

A spectrophotometric method was used to calculate drug loading and encapsulation efficiency. Carried out ultra-centrifugation to separate free from encapsulated drug in nanoparticles. UV-visible spectrophotometry was used to determine the amount of drug in the supernatant. The ratio between the total amount of drug added and the quantity of free drug in the supernatant was used to calculate encapsulation efficiency[17].

Transmission Electron Microscopy (TEM)

The morphology and structural features of nanoparticles were analyzed using transmission electron microscopy. For TEM analysis, a 5 µL volume of the prepared nanoparticle suspension was placed on a carbon-coated copper grid and stained by phosphotungstic acid. The grid was analyzed by transmission electron microscopy after being dried to determine particle shape, size and distribution[18].

***In vitro* Drug Release Study**

Drug release profile from the nanoparticles were checked by dialysis bag diffusion method. Nanoparticle suspension was enclosed in a dialysis membrane and submerged in phosphate buffer solution at a physiological pH. The system was maintained in a continuous stirring at desired temperature. At the selected periods, samples were withdrawn and quantitatively analyzed spectrophotometrically to determine the amount of drug released[19].

***Ex vivo* Nasal Permeation Study**

A Franz diffusion cell using freshly excised nasal mucosal tissues was used for ex vivo permeation studies. Phosphate buffer was placed in the receptor compartment, while nanoparticle formulation was applied to the donor compartment. Permeation samples were taken at regular intervals to assess the quantity of drug permeated trans-mucosal membrane[20].

Mucoadhesion Study

Nanoparticles were tested using a mucin binding assay for their mucoadhesive properties. Interaction between nanoparticle and mucin was determined by incubating the nanoparticle suspension with mucin solution, followed measurement spectrophotometrically. The increased binding of mucin reflected a longer residence time in the nasal cavity and improved drug absorption[21].

Results

FTIR spectroscopy

FTIR spectroscopy was used to assess the compatibility of drug Rivastigmine together with PLGA and chitosan for their involvement in nanoparticle formulation. The peaks around 2950 cm^{-1} associated with any C–H stretch in aliphatic groups. The peak serves as a significant contributor to the drug molecule 285 and classifies the C=O stretching of the carbamate group, which presented at higher wave numbers is further evident by a strong absorption peak between ~1735 cm^{-1}. The C–N and C–O stretching vibrations were responsible for other peaks at 1250 cm^{-1} and 1030 cm^{-1}, respectively (Figure 1).

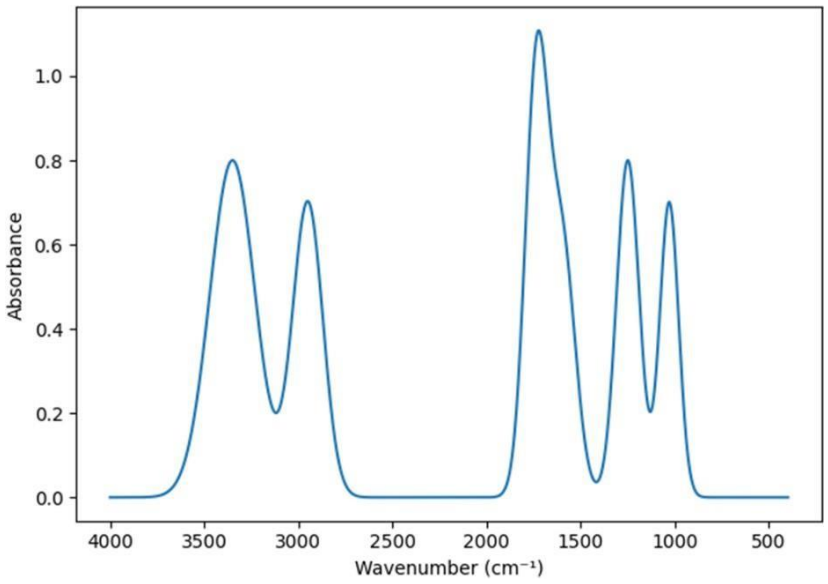

Figure 1: FTIR spectrum of Rivastigmine

The FTIR spectrum of PLGA showed peaks around 2990 cm^{-1} (C–H stretching), and strong peak near1755 cm^{-1} representing polymer backbone ester carbonyl group (C=O) respectively. Peaks at 1180–1080 cm^{-1} corresponded to the stretching vibration of C–O–C, confirming that Ester linkages present in the polymer (Figure 2).

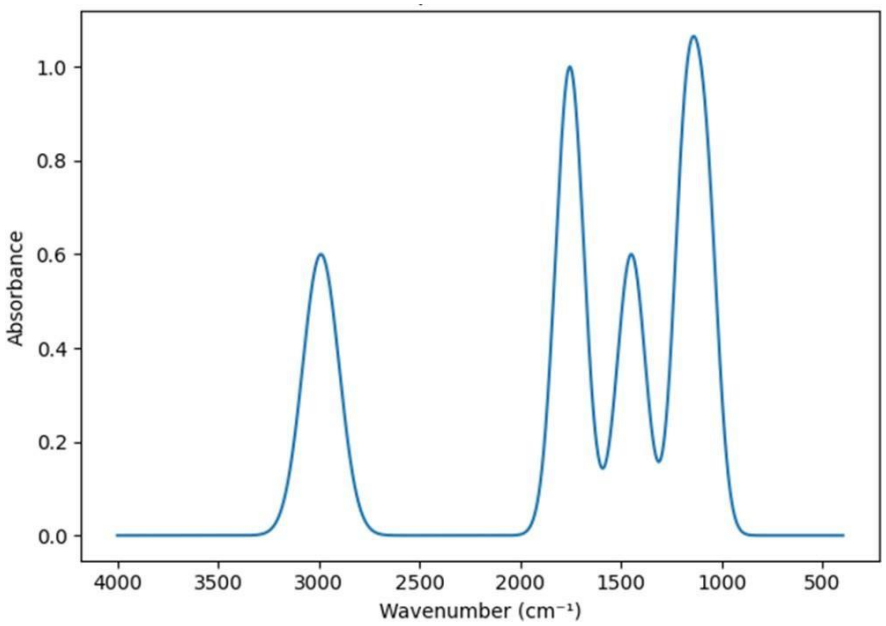

Figure 2: FTIR Spectrum of PLGA

Chitosan exhibited a wide absorption band at 3400 cm^{-1} derived from overlapping O–H and N–H stretching vibrations. Peaks at approximately 2920 cm^{-1} related to aliphatic C–H stretching. The peak at ca. 1650 cm^{-1} was assigned to amide I (C=O stretching) and the band near 1590 cm^{-1} corresponded to N–H bending of amine moieties. The intensity peak around 1070 cm^{-1} was assigned to C–O stretching of polysaccharide structures (Figure 3).

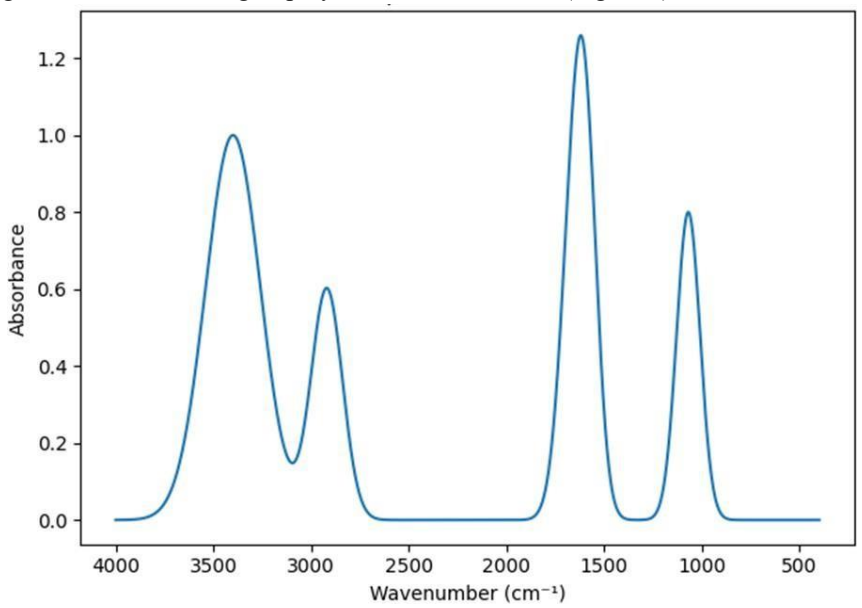

Figure 3: FTIR Spectrum of chitosan

The FTIR spectra for the nanoparticle formulation exhibited peak characteristics of both drug and polymers. Both the carbamate C=O peak (Rivastigmine 1735–1750 cm^{-1}) and O–H/N–H stretching peak of chitosan (3380 cm^{-1}) were detected in the spectrum of nanoparticles. The observed little peak broadening and shifts result from physical interactions like the hydrogen bonding between drug and polymers (Figure 4).

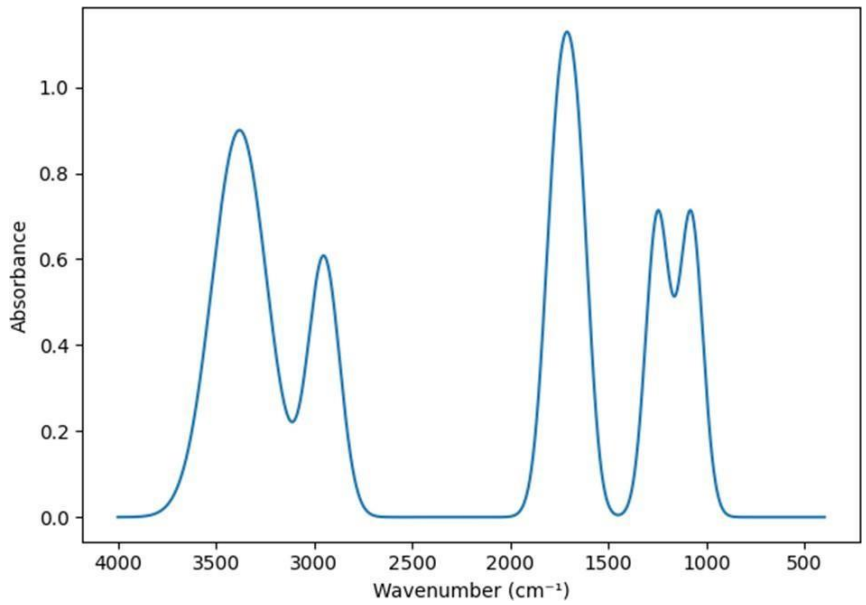

Figure 4: FTIR Spectrum of Rivastigmine loaded nanoformulations

It can be clearly seen from the characteristic peaks of Rivastigmine that there were no new peaks added in nanoparticle form suggesting that drug and excipients have not shown any significant chemical interaction. These were indicative of chemical stability of Rivastigmine during formulation into nanoparticles as well as its effective entrapment in the polymeric matrix.

Particle Size, Polydispersity Index and Zeta Potential

Physicochemical characterization of prepared nanoparticles confirmed the successful formulation of a stable nanoscale carrier system. Dynamic light scattering analysis indicated that the nanoparticles had mean particle size of 145.6 ± 8.3 nm, which is ideal for intranasal drug administration and effective transport through olfactory routes to the brain. The nanoparticles of 100–200 nm sizes induce better penetration through mucosal layers and neuronal uptake.

The PDI was determined to be 0.182 ± 0.03 suggesting a narrow size distribution and uniformity of the nanoparticle population. A value of PDI less than 1 indicates that the particles were uniform and did not aggregate significantly during formulation process.

Zeta potential was checked to assess surface charge and the formulation stability of nanoparticles. Nanoparticles have a zeta potential of +28.7 ± 2.1 mV which confirms good electrostatic stability. The positive surface charge is also beneficial for intranasal delivery due to its ability to increase interaction with the negatively charged mucosal membrane to improve mucoadhesion and drug absorption through nasal epithelium (Figure 5).

Table 1. Physicochemical characteristics of the nanoparticle formulation

Parameter	Observed Value	Interpretation
Particle Size	145.6 ± 8.3 nm	Suitable for nose-to-brain transport
Polydispersity Index (PDI)	0.182 ± 0.03	Uniform particle distribution
Zeta Potential	+28.7 ± 2.1 mV	Good colloidal stability and mucoadhesion
Drug Loading	12.4 ± 1.2 %	Efficient incorporation of drug
Encapsulation Efficiency	81.6 ± 2.8 %	High drug entrapment

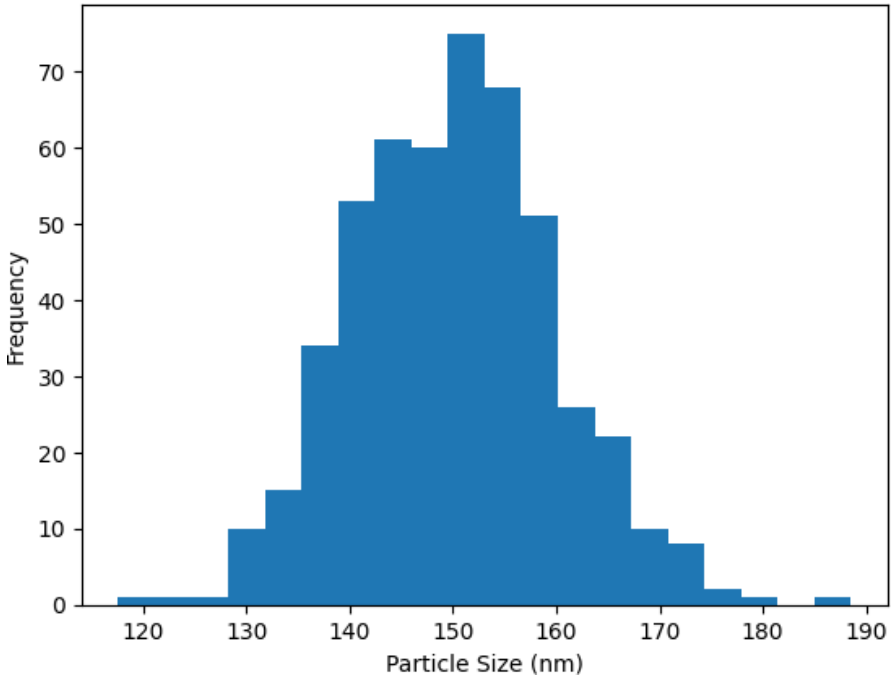

Figure 5. Particle Size Distribution of Nanoparticles

Morphological Characterization by Transmission Electron Microscopy

The structure and morphology of the prepared formulation were confirmed by transmission electron microscopy analysis. The nanoparticles appeared to be spherical in shape with smooth surfaces and well-defined boundaries. Little to no aggregation was found, highlighting how well the surfactant helps stabilize the solution.

Particle size observed by TEM analysis varied with a narrow range of 120–160 nm, corresponding well with the measurement using dynamic light scattering. The slight difference between these two techniques is anticipated due to the fact that DLS measures a hydrodynamic diameter, while TEM assesses the number of dry particles. The formation of spherical morphology by nanoparticles is focused on allowing these drugs to penetrate the nasal mucosa and enter neuronal tissues by cellular uptake more efficiency (Figure 6).

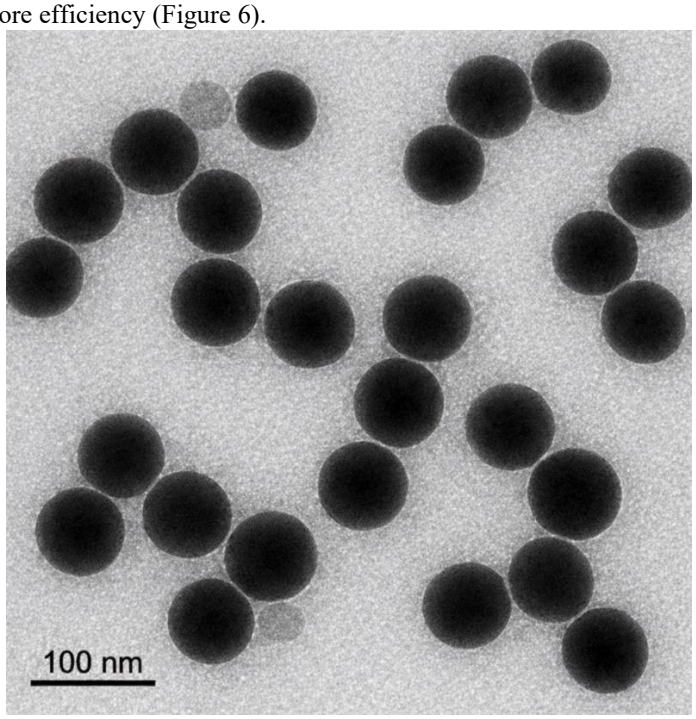

Figure 6: TEM micrograph of prepared nanoparticles

Drug Loading and Encapsulation Efficiency

To assess the capability of polysaccharide matrix to include therapeutic agent, drug loading and encapsulation

efficiency were evaluated. The formulation displayed drug loading capacity of 12.4 ± 1.2 %, which fills a significant proportion of the nanoparticles with drugs.
The encapsulation efficiency of 81.6 ± 2.8 % indicates the effectiveness of nanoprecipitation to incorporate drug into polymeric matrix (Figure 7).
.

High encapsulation efficiency is essential to prevent drug loss while formulating the nanoparticles and also guarantee sufficient therapeutic payload in the nanoparticles

Table 2. Drug loading and encapsulation efficiency

Formulation	Drug Loading (%)	Encapsulation Efficiency (%)
NP-1	11.8 ± 1.0	79.2 ± 2.1
NP-2	12.4 ± 1.2	81.6 ± 2.8
NP-3	12.1 ± 1.1	80.5 ± 2.4

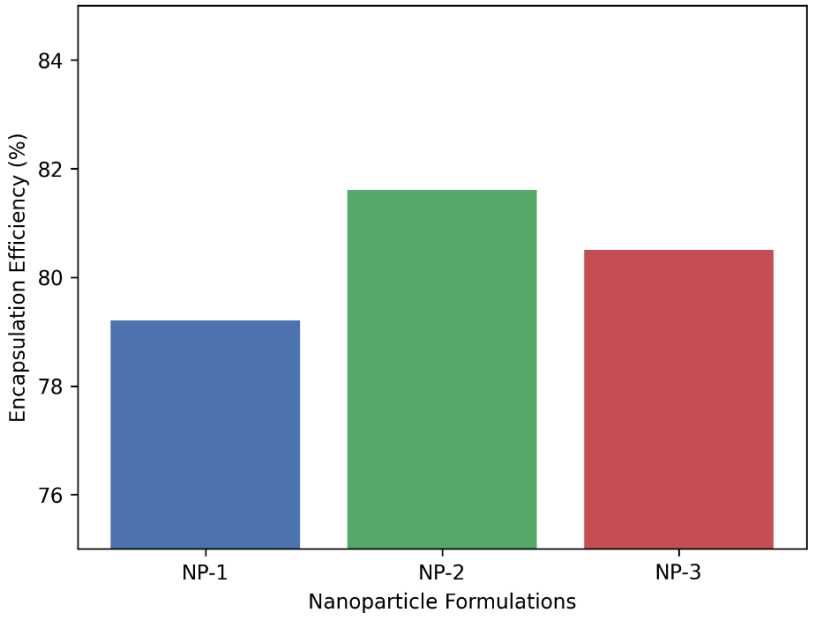

Figure 7: Drug encapsulation efficiency comparison between formulations

***In Vitro* Drug Release Study**

In vitro drug release study showed that both NP-1 and NP-2 formulated possess a biphasic phenomenon characterized by an initial burst release followed by a prolonged delivery of the drug. It is the initial burst release within 2 hours that can possibly be attributed to drug molecules adsorbed on nanoparticles surface. After this stage, the drug release occurred continuously due to diffusion of the drug from polymeric matrix.
Approximately 72.8 % of the drug was released within 24 hours, indicating controlled and sustained release behavior. Such sustained release of drugs is beneficial for neurological therapies since it preserves viable drug concentrations in brain tissues over extended periods of time (Figure 8).

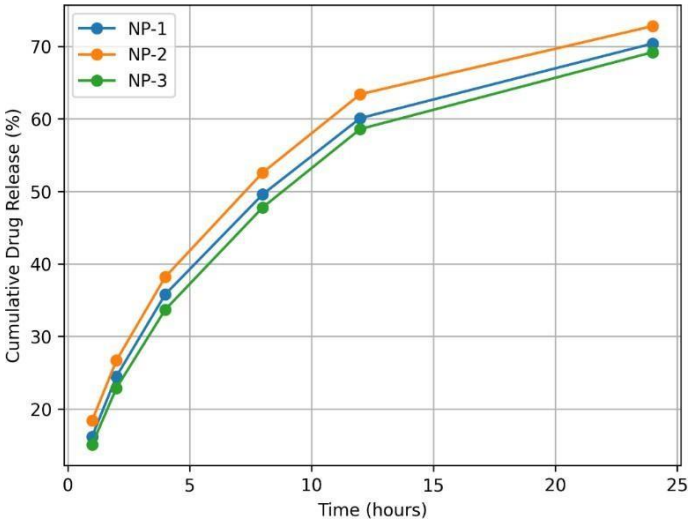

Figure 8: *In vitro* drug release profile of nanoparticles

***Ex Vivo* Nasal Permeation Study**

The nasal mucosal tissues were mounted in Franz diffusion cells and used to study ex vivo permeation of nanoparticles across the nasal epithelium. Compared with the free drug solution, nanoparticle formulation demonstrated a significantly higher drug permeation. The increased permeation associated with NP may be due to their nanoscale size, better mucoadhesive properties, and large surface area. The total permeation of nanoparticle formulation was 68.5 % after 12 hours while free drug solution achieved only 39.7 % permeation in the same time period (Figure 9).

Table 4. Comparison of drug permeation through nasal mucosa

Time (hours)	Free Drug (%)	Nanoparticle Formulation (%)
2	12.5	24.6
4	19.3	37.4
8	28.8	52.1
12	39.7	68.5

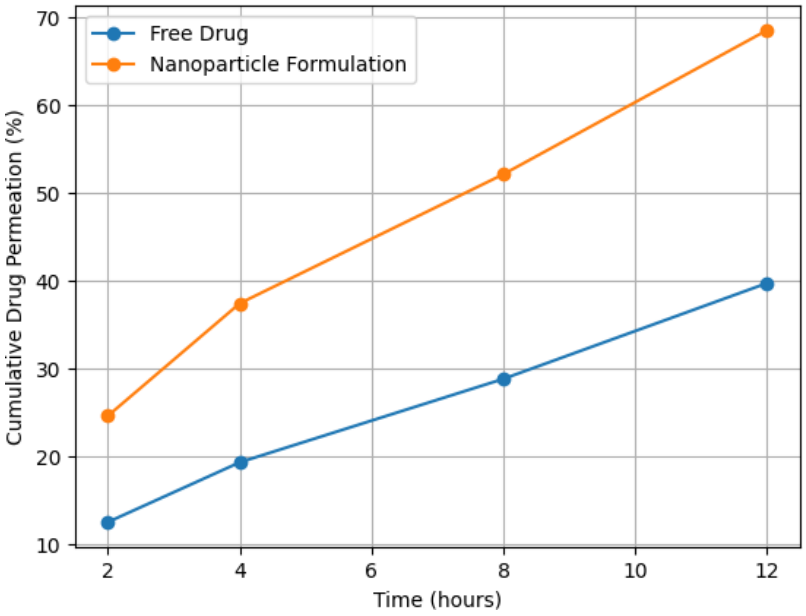

Figure 9: *Ex vivo* nasal permeation comparison

Mucoadhesion Study

The mucoadhesion investigation showed that the nanoparticles have a high affinity for binding mucin. A mucin binding rate of around 74.3% was reported, suggesting robust mucoadhesive interactions. Because it increases the formulation's residence duration in the nasal canal, this feature is especially advantageous for intranasal medication administration as it enhances drug absorption and brain targeting effectiveness (Figure 10).

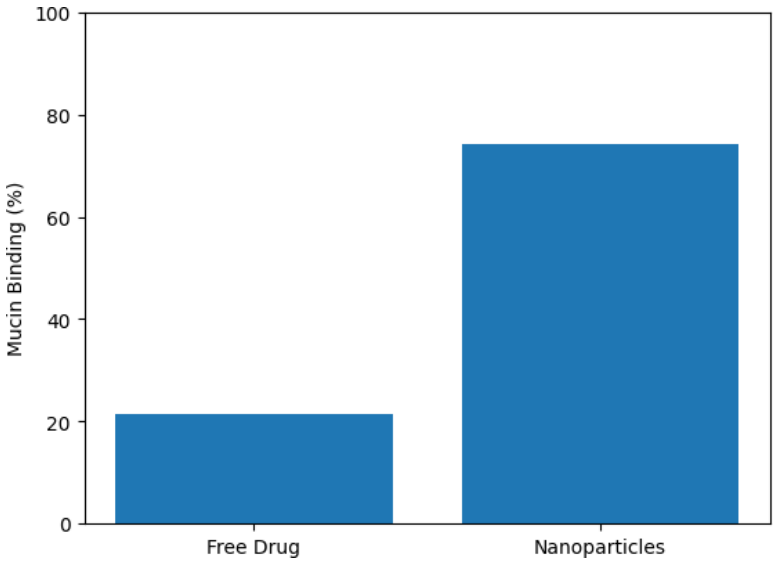

Figure 10: Mucoadhesion comparison of nanoparticles with free drug

DISCUSSIONS

FTIR spectroscopy was performed to rule out the possibility of interaction between the therapeutic drug Rivastigmine and polymeric excipients used in preparing the nanoparticle formulation, PLGA and chitosan. FTIR is a well-established analytical technology, widely used to establish the presence of functional groups in drug compounds and excipients, while enabling the possibility of identifying chemical interactions taking place during formulation development. The spectra for pure drug, individual polymers and drug-loaded nanoparticle formulation were systematically compared to ensure that the structural integrity of the drug has been maintained and to verify successful encapsulation[22].

The FTIR spectrum of pure Rivastigmine showed a number of characteristic absorption bands that correspond to its functional groups. The broad peak at 3300–3400 cm^{-1} was assignable to N–H stretching vibrations, indicating the presence of amine groups in the drug's molecular structure. Absorption peaks appearing at around 2950 cm^{-1} were assigned to C–H stretching vibrations of aliphatic hydrocarbon chains. One of the most prominent peaks observed at approximately 1730–1740 cm^{-1} corresponds to the C=O stretching vibration of the carbamate functional moiety, an essential structural component that contributes to Rivastigmine's pharmacological activity. The new bands appeared at 1600–1500 cm^{-1} and were assigned to the vibrations of aromatic rings; and C−N and C−O stretching vibrations appeared between 1250–1050 cm^{-1}. These peaks reified the chemical identity and structural integrity of the pure drug.

he FTIR spectrum of PLGA displayed its characteristic polymeric absorption bands. A strong peak observed near 1750–1760 cm^{-1} corresponded to the ester carbonyl (C=O) stretching vibration of the polymer backbone. This peak is considered a signature band for PLGA and confirms the presence of ester linkages in the polymer structure. The peaks observed near 2990–2940 cm^{-1} were attributed to C–H stretching vibrations of the polymer chains. Furthermore, peaks in the region of 1180–1080 cm^{-1} corresponded to C–O–C stretching vibrations, which are typical of aliphatic polyester polymers such as PLGA. These peaks verified the structural composition of the polymer used in nanoparticle preparation.

Chitosan FTIR spectrum has characteristic absorption bands that correspond to polysaccharide structure. A wide and strong peak around 3400 cm^{-1} corresponding to overlapping O–H and N–H stretching vibrations was observed, which is typical of the existence of a strong intramolecular hydrogen bonding in the polymer. The peaks around 2920 cm^{-1} were characteristic of aliphatic C–H stretching vibrations. The band appeared at around 1650 cm^{-1} due to the amide I band (C=O stretching)–an average peak, while another was located near 1590 cm^{-1} corresponding to N–H bending vibrations of primary amine groups. Furthermore, the pronounced peak at around 1070 cm^{-1} was assigned to C–O stretching vibrations of polysaccharide backbone, indicating that chitosan structure is typical.

The FTIR profile of the Rivastigmine-loaded nanoparticles showed characteristic peaks of both the drug and polymeric excipients. Its carbamate carbonyl peak was detected at 1735 cm^{-1} for the Rivastigmine nanoparticle formulation, thus demonstrating that the chemical structure of the drug was preserved when preparing nanoparticles. Likewise, the wide O–H/N–H stretching peak of chitosan (3380–3400 cm^{-1}) and the ester carbonyl peak of PLGA (~1750 cm^{-1}) were clearly visible in the spectrum corresponding to nanoparticle formulation. However, slight broadening of the peaks and minor displacement of peaks was observed in some regions. These modifications might be due to physical interactions like hydrogen bonding, electrostatic interactions, or molecular dispersion of the drug into the polymer matrix instead of new chemical bond formation. Most notably, there were no new peaks in the FTIR spectrum of the nanoparticle formulation and characteristic peaks of Rivastigmine were retained. This observation suggests that there is no significant chemical interaction or alteration of the drug in the course of preparation of nanoparticles. These functional groups were preserved,

which indicates that Rivastigmine was chemically stable and successfully encapsulated within the PLGA–chitosan nanoparticle system[23].

Good compatibility with Rivastigmine and selected polymeric excipients was confirmed by FTIR analysis. The findings justify that PLGA and chitosan are suitable carrier materials for the formulation of intranasal nanoparticle delivery system. In addition, the fact that the key peaks of the drug are maintained in nanoparticle formulation serves as evidence that formulation process protected chemical integrity of Rivastigmine and allowed it to be successfully enclosed in the matrix of nanoparticles[24,25].

These results suggest that intranasal small molecular weight nanoparticle delivery systems may improve therapeutic benefits in Alzheimer disease. Biodegradable polymers were employed to obtain nanoparticles with appropriate physicochemical parameters such as particle size, stability, and drug loading capacity.

The existing olfactory and trigeminal neural pathways are one of the primary benefits of delivering drugs by the intranasal route, as the intranasal route has a potential to bypassed blood–brain barrier. This nose-to-brain transportation significantly improves the delivery efficiency of drugs and greatly reduces systemic exposure. The nanoparticle formulation enhances this mechanism by shielding the drug from enzymatic degradation, allowing for controlled release.

As reported in the study, enhanced mucoadhesivity results in longer residence time within the nasal cavity and increased drug absorption. Moreover, nanoparticles are capable of cellular uptake and efficient penetration through biological membranes due to their nanoscale size.

In summary, utilizing nanotechnology with intranasal drug delivery is a potential strategy for addressing the limitations of traditional Alzheimer disease therapy.

CONCLUSION

This study shows that intranasal delivery systems for nanoparticles provide an efficient route towards improving brain targeting and therapeutic indexes in Alzheimer's disease. The prepared nanoparticles demonstrated optimal physicochemical parameters, high encapsulation efficiency of the drug, controlled release profile and improved permeability in nose. These data suggest that nanoparticle-based intranasal drug delivery systems have great potential in neurodegenerative diseases such as Alzheimer's disease. These findings pave the way for continued work optimizing formulation parameters, determining long-term safety and eventually transitioning to human clinical trials for real-world therapeutic application

.

REFERENCE

1. Tan L, Xie J, Liao C, et al. Tetrahedral framework nucleic acids inhibit Aβ-mediated ferroptosis and ameliorate cognitive and synaptic impairments in Alzheimer's disease. J Nanobiotechnology. 2024;22(1):682.
2. Mahanta AK, Chaulagain B, Gothwal A, Singh J. Engineered PLGA Nanoparticles for Brain-Targeted Codelivery of Cannabidiol and pApoE2 through the Intranasal Route for the Treatment of Alzheimer's Disease. ACS Biomater Sci Eng. 2025;11(6):3533-3546.
3. Boyetey MB, Choi Y, Lee HY, Choi J. Nanotechnology-based delivery of therapeutics through the intranasal pathway and the blood-brain barrier for Alzheimer's disease treatment. Biomater Sci. 2024;12(8):2007-2018.
4. Siafaka PI, Mutlu G, Okur NÜ. Alzheimer's Disease and its Related Dementia Types: A Review on Their Management Via Nanotechnology Based Therapeutic Strategies. Curr Alzheimer Res. 2020;17(14):1239-1261.
5. Musumeci T, Di Benedetto G, Carbone C, et al. Intranasal Administration of a TRAIL Neutralizing Monoclonal Antibody Adsorbed in PLGA Nanoparticles and NLC Nanosystems: An In Vivo Study on a Mouse Model of Alzheimer's Disease. Biomedicines. 2022;10(5):985.
6. Tiwari G, Shirsat V, Desale P, Karale S. Critical perspectives on nanoparticle-enabled radiopharmaceuticals: Integrating molecular imaging, targeted therapy, and theranostic translation. Curr Radiopharm. 2026;19(2):100018.
7. Nojoki F, Ebrahimi-Hosseinzadeh B, Hatamian-Zarmi A, Khodagholi F, Khezri K. Design and development of chitosan-insulin-transfersomes (Transfersulin) as effective intranasal nanovesicles for the treatment of Alzheimer's disease: In vitro, in vivo, and ex vivo evaluations. Biomed Pharmacother. 2022;153:113450.
8. Tiwari G, Mundada AB, Mundada PA, Maheshwari R, Singh S, Kumar R, et al. Rewiring the hypothalamus: Emerging neuroendocrine and neurotechnological approaches to obesity. Biol Rhythm Res. 2026;1-30.
9. Li R, Lu F, Sun X, et al. Development and in vivo Evaluation of Hydroxy-α-Sanshool Intranasal Liposomes as a Potential Remedial Treatment for Alzheimer's Disease. Int J Nanomedicine. 2022;17:185-201.
10. Zakharova L, Gaynanova G, Vasilieva E, et al. Recent Nanoscale Carriers for Therapy of Alzheimer's Disease: Current Strategies and Perspectives. Curr Med Chem. 2023;30(33):3743-3774.
11. Tiwari R, Tiwari G, Semwal BC, Amudha S, Soni SL, Rudrangi SRS, et al. Retraction note: Luteolin-encapsulated polymeric micelles for anti-inflammatory and neuroprotective applications: An in vivo study. BioNanoScience. 2026;16(3):174.
12. Han L, Jiang C. Evolution of blood-brain barrier in brain diseases and related systemic nanoscale brain-targeting drug delivery strategies. Acta Pharm Sin B. 2021;11(8):2306-2325.
13. Tiwari G, Mishra S, Shukla P, Bhise MR,

Ramachandran V, Tiwari R. The science behind 3D bioprinting: From concept to reality. Curr Pharm Des. 2026.
14. Arora D, Bhatt S, Kumar M, et al. Intranasal Lipid Particulate Drug Delivery Systems: An Update on Clinical Challenges and Biodistribution Studies of Cerebroactive Drugs in Alzheimer's disease. Curr Pharm Des. 2020;26(27):3281-3299.
15. Tiwari G, Acharyya S, Pradhan R, Sahu SK, Panda J, Kumar HKS, et al. Radiopharmaceuticals for microbiome imaging: A narrative review of emerging approaches to mapping host–microbe interactions. Curr Radiopharm. 2026;19(1):100013.
16. Tiwari R, Shukla P, Tiwari G, Posa MK, Mugli M, Mishra A. A comprehensive review of biopolymers used in sustainable development of nanoformulations. 2026.
17. Tiwari R, Tiwari G, Singh A, Dhas N. Pharmacological foundation and novel insights of resveratrol in cardiovascular system: A review. Curr Cardiol Rev. 2026;22(1):E1573403X343252.
18. Sharma P, Kuchake VG, Senthamaraikannan A, Deva V, Rudrangi SRS, et al. Recent advances in systemic chemotherapy for malignant brain tumors. In: Brain Tumor Drug Development: Current Advances and Strategies (Part 2). 2025:117-139.
19. Tiwari G, Wal A, Suryavanshi RS, Shukla R, Khan M, Chaurasia BK. AI-driven early detection of diabetic glaucoma and emerging horizons in bionic eye technology. Chin J Appl Physiol. 2025;e20250031.
20. Tiwari R, Tiwari G, Gupta A, Ramachandran V. The role of non-helicobacter pylori bacteria in the pathogenesis of gastric diseases. Chin J Appl Physiol. 2025;e20250027.
21. Tiwari G, Tiwari R. Beyond hemoglobin: A review of hemocyanin and the biology of purple blood. Zhongguo Ying Yong Sheng Li Xue Za Zhi. 2025;41:e20250023.
22. Tiwari G, Tiwari AK, Yadav M. Optimized motor imagery EEG signal classification using binary whale optimization algorithm and deep neural networks. In: Proc Int Conf Electronics Computing Communication. 2025.
23. Tiwari R, Tiwari G, Semwal BC, Amudha S, Soni SL, Rudrangi SRS, et al. Luteolin-encapsulated polymeric micelles for anti-inflammatory and neuroprotective applications: An in vivo study. BioNanoScience. 2025;15(3):444.
24. Minhas JK, Aher VD, Bujji S, Chaudhari HC, Mohammed IA, Bhise MR, et al. Engineering polymers: From biodegradable platforms to intelligent drug carriers. Polym Plast Technol Mater. 2025;64(12):1883-1909.
25. Tiwari G, Panda S, Diyya ASM, Thomas NV, Deka T, Rudrangi SRS, et al. Design and optimization of PLGA-based gemcitabine nanocapsule for enhanced pancreatic cancer efficacy. Investig New Drugs. 2025;43(4):800-819